Amplification of terahertz radiation in carbon nanotubes

7 authors, including:

Samuel Yeboah Mensah
University of Cape Coast
88 PUBLICATIONS   **383** CITATIONS

SEE PROFILE

N. G. Mensah
University of Cape Coast
54 PUBLICATIONS   **258** CITATIONS

SEE PROFILE

K. A. Dompreh
University of Cape Coast
43 PUBLICATIONS   **102** CITATIONS

SEE PROFILE

Anthony Twum
University of Cape Coast
21 PUBLICATIONS   **43** CITATIONS

SEE PROFILE

Some of the authors of this publication are also working on these related projects:

Study of Acoustic effects in Carbon Allotropes View project

IMRT with telecobalt machine using forward planning View project

THE EUROPEAN
PHYSICAL JOURNAL B

Regular Article

Amplification of terahertz radiation in carbon nanotubes

Sulemana S. Abukari[1], Kofi W. Adu[2,3,a], Samuel Y. Mensah[1], Natalia G. Mensah[4,5], Kwadwo A. Dompreh[1], Anthony Twum[1], and Musah Rabiu[6]

[1] Department of Physics, Laser and Fibre Optics Centre, University of Cape Coast, Cape Coast, Ghana
[2] Department of Physics, The Pennsylvania State University, Altoona College, Altoona, Pennsylvania 16601, USA
[3] Materials Research Institute, The Pennsylvania State University, University Park, Pennsylvania 16802, USA
[4] National Centre for Mathematical Sciences, Ghana Atomic Energy commission, Kwabenya, Accra, Ghana
[5] Department of Mathematics, University of Cape Coast, Cape Coast, Ghana
[6] Department of Applied Physics, University for Development Studies, Navorongo, Ghana

Abstract. We investigate theoretically the feasibility of amplification of terahertz radiation in aligned achiral carbon nanotubes, a zigzag (12,0) and an armchair (10,10) in comparison with a superlattice using a combination of a constant direct current (dc) and a high-frequency alternate current (ac) electric fields. The electric current density expression is derived using the semiclassical Boltzmann transport equation with a constant relaxation time. The electric field is applied along the nanotube axis. Analysis of the current density versus electric field characteristics reveals a negative differential conductivity behavior at high frequency, as well as photon assisted peaks. The photon assisted peaks are about an order of magnitude higher in the carbon nanotubes compared to the superlattice. These strong phenomena in carbon nanotubes can be used to obtain domainless amplification of terahertz radiation at room temperature.

1 Introduction

Terahertz (THz) region of the electromagnetic (EM) spectrum refers to the frequency range between the mid-infrared and the microwave region (0.3 THz−10 THz). This EM region has a lot of promising applications in various areas of science and technologies include astronomy, broadband communication, pollution monitoring, poisonous gas sensing, etc. [1,2]. In spite of the potential applications, this region of the EM spectrum is yet to be fully exploited, due to the limited availability of device sources and detectors [3]. Over the past decade, terahertz science and technology has advanced considerably with both optical-bench-based systems and solid state quantum cascade lasers [3]. The main drawback of these quantum cascade THz sources is low working temperatures, making it difficult to maintain population inversion at room temperature [4]. So far the highest temperature attained for a THz source operating at 3 THz frequency is 160 K [5]. Creating a compact reliable source of THz radiation that could operate at room temperature still remains one of the most formidable challenges of contemporary applied physics. Most recently, carbon nanotube has been identified for THz technology due to its superb physical properties. Different proposals of carbon nanotubes for THz applications have been made; that ranges from multipliers [1,6], amplifies [7], switches [8] to antennas [9].

Carbon nanotube (CNT) is a single layer nanometer-size cylinder made of carbon atoms. The cylinder has no bulk atoms, only surface atoms. It is a layer of graphene seamlessly rolled into a cylinder. CNTs have intriguing physical properties (mechanical, electrical, optical, etc.) due to their unique structure; combine with the one-dimensional solid state characteristics [10]. These properties depend on the fundamental indices (n, m) of the CNT. The indices (n, m) specify the diameter and the chiral angle of the CNT. As n and m vary, conduction ranges from metallic to semiconducting [11], with $n = m$ been metallic and $m = 0$ been semiconducting. The band gap of the semiconducting CNTs has an inverse diameter (d) dependent, ranging from 0.2 eV to 2 eV with $E_g \approx 0.9/d$ nm [12], where $d = a_0 \ (n^2 + m^2 - nm)^{1/2}/\pi$ is the nanotube diameter and $a_0 = 0.246$ nm is graphene lattice constant. The peculiarity of CNTs (e.g., strong nonparabolic dispersion law) raises the question of whether these structures could be used for high-order harmonic generation [13,14]. Different theoretical models and experimental techniques are being pursued to demonstrate the feasibility of using CNT for THz applications [15–19]. These range from THz generation Cherenkov-type emitters based on hot electrons in quasimetallic CNT ($n - m = p$ with p as a non-zero interger), frequency multiplication in chiral-nanotube-based superlattices controlled by a transverse electric field, and THz radiation detection and emission by armchair nanotubes in a strong magnetic field [15], ab initio

[a] e-mail: cxa269@psu.edu

molecular dynamic simulations [16], CNT capacitor circuit model [17], impedance transmission model [18], effective conductivity model [19], just to mention a few.

Nonlinearity of the current density characteristics of CNTs gives rise to generation of harmonics of microwaves and direct current (dc) generation, as well as terahertz generation [1,20,21]. However, Bloch oscillations of electrons within the CNTs cause an appearance of negative differential conductivity (NDC) for dc fields larger than the critical electric field [14]. This leads to electric current instabilities and formation of domains in the CNTs [22]. These current instabilities are destructive to the formation of the terahertz frequency. Therefore, it is important to consider the scheme of generation of terahertz radiation that can suppress electric instabilities while preserving high-frequency gain at room temperature. Theoretical realizations of superlattice oscillators (SL) with ac bias have been reported [23–25], that demonstrated domainless amplification of terahertz radiation. However, there are limited reports of such effects in CNTs, especially simultaneous utilization of dc-ac electric fields. In this report, we present a theoretical investigation of a (12,0)-zigzag single wall carbon nanotube (z-SWCNT) and a (10,10)-armchair single wall carbon nanotube (a-SWCNT) in comparison with superlattice (SL), stimulated with a time dependent dc-ac electric fields for THz frequency amplification at room temperature. Our results reveal an order of magnitude effective suppression of the electric instability in the one dimensional CNTs in comparison with the two-dimensional SL [23–25].

2 Theoretical model

Following the approach of references [15–17], we consider an undoped achiral CNTs (i.e., (12,0)-zigzag and (10,10) armchair) exposed simultaneously to a dc-ac electric field.

$$E(t) = E_0 + E_1 \cos \omega t \qquad (1)$$

where E_0 is the constant electric field, E_1 and ω are the amplitude and the frequency of the ac field, respectively. The investigation is done within the semiclassical approximation in which conduction electrons with energy below the energy of the interband transitions move in the crystalline lattice like free quasi-particles with dispersion law extracted from quantum theory. Taking into account the hexagonal crystalline structure of a rolled graphene in a form of CNT and using the tight binding approximation, the energy dispersion for z- and a-SWCNTs are expressed as in equations (2) and (3), respectively [1]:

$$\varepsilon(s\Delta p_\varphi, p_z) \equiv \varepsilon_s(p_z) = \pm\gamma_0 \left[1 + 4\cos(ap_z) \right.$$
$$\left. \times \cos\left(\frac{a}{\sqrt{3}} s\Delta p_\varphi\right) + 4\cos^2\left(\frac{a}{\sqrt{3}} s\Delta p_\varphi\right) \right]^{1/2}$$
$$(2)$$

$$\varepsilon(s\Delta p_\varphi, p_z) \equiv \varepsilon_s(p_z) = \pm\gamma_0 \left[1 + 4\cos(as\Delta p_\varphi) \right.$$
$$\left. \times \cos\left(\frac{a}{\sqrt{3}} p_z\right) + 4\cos^2\left(\frac{a}{\sqrt{3}} p_z\right) \right]^{1/2} \quad (3)$$

where $\gamma_0 \sim 3.0$ eV is the overlapping integral, p_z is the axial component of quasimomentum, Δp_φ is transverse quasimomentum level spacing and s is an integer. The expression for a in equations (2) and (3) is given as $a = 3b/2\hbar$, $b = 0.142$ nm is the C-C bond length. The $-$ and $+$ signs correspond to the valence and conduction bands, respectively. Due to the transverse quantization of the quasi-momentum, its transverse component can take n discrete values, $p_\varphi = s\Delta p_\varphi = \pi\sqrt{3}/an$ ($s = 1, \ldots, n$). Unlike transverse quasimomentum p_φ, the axial quasimomentum p_z is assumed to vary continuously within the range $0 \leqslant p_z \leqslant 2\pi/a$, which corresponds to the model of infinitely long CNT ($L = \infty$). This model is applicable to the case under consideration because of the restriction to the temperatures and /or voltages well above the level spacing [1,11], i.e. $k_B T > \varepsilon_C, \Delta\varepsilon$, where k_B is Boltzmann constant, T is the temperature, ε_C is the charging energy. The energy level spacing $\Delta\varepsilon$ is given by

$$\Delta\varepsilon = \pi\hbar\upsilon_F/L \qquad (4)$$

where υ_F is the Fermi velocity and L is the carbon nanotube length [5].

Employing Boltzmann transport equation with a single relaxation time approximation,

$$\frac{\partial f(p)}{\partial t} + eE(t)\frac{\partial f(p)}{\partial P} = -\frac{[f(p) - f_0(p)]}{\tau} \qquad (5)$$

where e is the electron charge, $f_0(p)$ is the equilibrium distribution function, $f(p, t)$ is the distribution function, and τ is the relaxation time. The time dependent electric field $E(t)$ is applied along the CNT axis. In this case the relaxation time τ is assumed to be constant. The relaxation term of equation (5) describes the effects of the dominant type of scattering (e.g. electron-phonon and electron-twistons). For the electron scattering by twistons (thermally activated twist deformations of the tube lattice), τ is proportional to m (armchair dual index (m, n), $m = n$) [26] and the I-V characteristics shows that scattering by twistons increases and decreases in the negative differential conductivity (NDC) region; the smaller m is, the stronger this effect. Quantitative changes of the I-V curves turn out to be insignificant in comparison with the case of $\tau = $ const. [25,27].

The distribution functions for zigzag CNT could be expanded in Fourier series [1] as,

$$f_0(p) = \Delta p_\varphi \sum_{s=1}^{n} \delta(p_\varphi - s\Delta p_\varphi) \sum_{r \neq 0} f_{rs} e^{iarp_z} \qquad (6)$$

and

$$f(p, t) = \Delta p_\varphi \sum_{s=1}^{n} \delta(p_\varphi - s\Delta p_\varphi) \sum_{r \neq 0} f_{rs} e^{iarp_z} \phi_\upsilon(t).$$
$$(7)$$

Here the energy unit $\hbar = 1$ has been used. $\delta(x)$ is the Dirac delta function, r is summation over the stark component, f_{rs} is the coefficient of the Fourier series and $\phi_v(t)$ is the factor by which the Fourier transform of the nonequilibrium distribution function differs from its equilibrium distribution counterpart. All other parameters are as defined above. The equilibrium distribution function $f_0(p)$ can be expanded in an analogous series with coefficient f_{rs} expressed as:

$$f_{rs} = \frac{a}{2\pi\Delta p_\varphi S} \int_0^{\frac{2\pi}{a}} \frac{e^{-iarp_z}}{1 + \exp\left(\varepsilon_s(p_z)/k_B T\right)} dp_z. \quad (8)$$

Substituting equations (6) and (7) into equation (5), and solving with equation (1) we obtain:

$$\phi_v(t) = \sum_{k=-\infty}^{\infty} \sum_{m=-\infty}^{\infty} \frac{J_k(r\beta) J_{k-v}(r\beta)}{1 + i(\Omega r + k\omega)\tau} \exp(iv\omega t) \quad (9)$$

where $\beta = \frac{eaE_1}{\omega}$, $J_k(\beta)$ is the Bessel function of the kth order and $\Omega = eaE_0$.

To obtain the current density, we expand $\varepsilon_s(p_z)/\gamma_0$ in Fourier series with coefficients ε_{rs}:

$$\frac{\varepsilon_s(p_s, s\Delta p_\varphi)}{\gamma_0} = \varepsilon_s(p_z) = \sum_{r\neq 0} \varepsilon_{rs} e^{iarp_z} \quad (10)$$

where

$$\varepsilon_{rs} = \frac{a}{2\pi\gamma_o} \int_o^{\frac{2\pi}{a}} \varepsilon_s(p_z) e^{-iarp_z}, \quad (11)$$

and expressing the velocity as

$$v_z(p_z, s\Delta p_z) = \frac{\partial \varepsilon_s(p_z)}{\partial p_z} = \gamma_o \sum_{r\neq 0} iar\varepsilon_{rs} e^{iarp_z}, \quad (12)$$

the surface current density is then defined as

$$j_z = \frac{2e}{(2\pi\hbar)^2} \iint f(p) v_z(p) d^2p$$

or

$$j_z = \frac{2e}{(2\pi\hbar)^2} \sum_{s=1}^n \int_0^{\frac{2\pi}{a}} f(p_z, s\Delta p_\varphi, \phi_v(t)) v_z(p_z, s\Delta p_\varphi) dp_z. \quad (13)$$

The integration is taken over the first Brillouin zone. Substituting equations (7), (9) and (12) into (13) we determined the current density for the zigzag CNT after averaging over a period of time t as:

$$j_z = \frac{8e\gamma_0}{\sqrt{3}\hbar na} i \sum_r r \sum_{s=1}^n f_{rs}\varepsilon_{rs}$$
$$\times \sum_{k=-\infty}^{\infty} \frac{J_k^2(r\beta)(1 - i(\Omega r + k\omega)\tau)}{1 + ((\Omega r + k\omega)\tau)^2}. \quad (14)$$

When the electric field amplitudes are small $\beta \ll 1$, we can use the Bessel function approximation $J_{\pm 1}^2 \sim (r^2\beta/2)^2$ and $J_0^2 \sim 1 - \frac{r^4\beta^2}{2}$. Hence from equation (14) we obtain real part of the current density to be,

$$j_z = j_0 \sum_{r=1}^{\infty} r^2 \sum_{s=1}^n f_{rs}\varepsilon_{rs}$$
$$\times \left(\frac{\left(1 + (\omega\tau)^2 - (\omega_B\tau r)^2\right)}{\left[1 + ((\omega_B r - \omega)\tau)^2\right]\left[1 + ((\omega_B r + \omega)\tau)^2\right]} \right) \quad (15)$$

and the imaginary part

$$j_z = j_0 \sum_{r=1}^{\infty} r \sum_{s=1}^n f_{rs}\varepsilon_{rs}$$
$$\times \left(\frac{i\omega\tau\left(1 - 3(\tau\omega_B r)^2 + (\omega\tau)^2\right)}{\left[1 + (\omega_B r\tau)^2\right]\left[1 + ((\omega_B r - \omega)\tau)^2\right]\left[1 + ((\omega_B r + \omega)\tau)^2\right]} \right) \quad (16)$$

where $j_0 = \frac{8e\gamma_0}{\sqrt{3}\hbar na}\left(\frac{(\omega_B r\tau)\beta^2}{2}\right)$ and $\omega_B = \Omega$. These expressions are similar to the equations obtained in reference [24] for $\beta \ll 1$. On the other hand we can re-write equation (14) in the form of reference [25] as:

$$j_z = j_0 \sum_{r=1}^{\infty} r \sum_{k=-\infty}^{\infty} J_k^2(r\beta) j_{dc}(\omega_B r + kE^*) \sum_{s=1}^n f_{rs}\varepsilon_{rs} \quad (17)$$

where $E^* = \frac{\hbar\omega}{a}$ and for $k \neq 0$, $j_{dc}(\omega_B r + kE^*)$ is the photon replicas.

Expression (17) is the superposition of the dc current density and its various photon replicas. We obtained the dc differential conductivity as:

$$\sigma_z = \frac{\partial j_z}{\partial E_0} = \sigma_o \sum_{r=1}^{\infty} r \sum_{k=-\infty}^{\infty} k j_k^2(r\beta)$$
$$\times \frac{\left(1 - (\omega_B r + kE^*)^2\right)}{\left(1 + (\omega_B r + kE^*)\right)^2} \sum_{s=1}^n f_{rs}\varepsilon_{rs}. \quad (18)$$
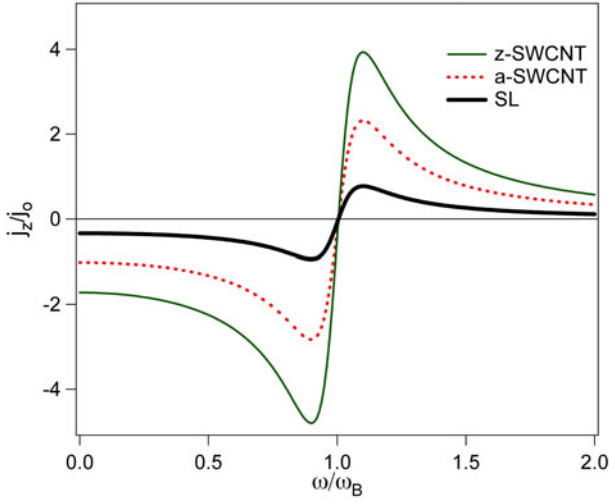
However, for a SL [27],

$$j_z = j_0 \sum_{k=-\infty}^{\infty} J_k^2(\beta) j_{dc}(\omega_B + kE^*) \quad (19)$$

and

$$\sigma_z = \frac{\partial j_z}{\partial E_0} = \sigma_o \sum_{k=-\infty}^{\infty} k j_k^2(\beta) \frac{\left(1 - (\omega_B + kE^*)^2\right)}{\left(1 + (\omega_B + kE^*)\right)^2} \quad (20)$$

where $\omega_B = eaE_0$ for the zigzag CNT and $\omega_B = eaE_0/\sqrt{3}$ for the armchair CNT and $\beta = eaE_1/\omega$. Comparing equations (17)−(20), it is evident that the 1D CNTs have the
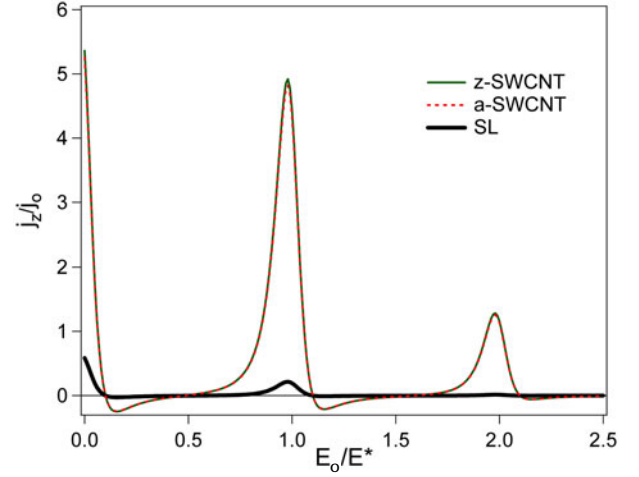
Fig. 1. j_z/j_0 vs. ω/ω_B curves for the superlattice (SL, thick solid black curve), the (10,10) armchair SWCNT (a-SWCNT, red dotted curve), and the (12,0) zigzag SWCNT (z-SWCNT, green thin solid curve) using $\tau = 3 \times 10^{-12}$ s and $T = 287.5$ K.

stark component (summation over r, Eqs. (17) and (18)) which is absent in SL (Eqs. (19) and (20)) [27]. The stark component and the specific dispersion law inherent in the hexagonal crystalline structure of the CNTs are responsible for the very high nonlinearity.

3 Results, discussion and conclusion

We present the results of a semiclassical theory of electron transport in achiral SWCNT (armchair (10,10) and zigzag (12,0)) exposed to dc-ac electric fields. The results are compared with that of a superlattice under similar conditions. The Boltzmann transport equation is solved in the framework of momentum-independent relaxation time. An analytical expression for the current density is obtained for the situation $\beta \ll 1$. The nonlinearity is analyzed using dependence of the current density on the frequency.

In Figure 1, we show the plots of the real part of the normalized high-frequency conductivity, j_z/j_o (Eqs. (17) and (19)) as a function of dimensionless frequency (ω/ω_B) for the superlattice (SL, thick solid black curve), the (10,10) armchair-SWCNT (a-SWCNT, red dotted curve) and the (12,0) zigzag-SWCNT (z-SWCNT, green solid thin curve), respectively. In all three systems, the real part of the differential conductivity is initially negative at zero frequency and becomes more negative with increasing frequency, until it researches a resonance minimum at a frequency just below the Bloch frequency $\omega_B \tau = 1.0$ and then turning positive (resonance enhancement) just below the Bloch frequency (Fig. 1). This resonance enhancement is indicative of terahertz gain at that frequency without the formation of current instabilities induced by negative dc conductivity. It is worth noting that the effect is about two times and three times stronger in the a-SWCNT and z-SWCNT, respectively, in comparison to

Fig. 2. j_z/j_0 vs. E_o/E^* curves for the superlattice (SL, thick solid black curve), the (10,10) armchair SWCNT (a-SWCNT, red dotted curve), and the (12,0) zigzag SWCNT (z-SWCNT, green thin solid curve) using $\tau = 3 \times 10^{-12}$ s and $T = 287.5$ K.
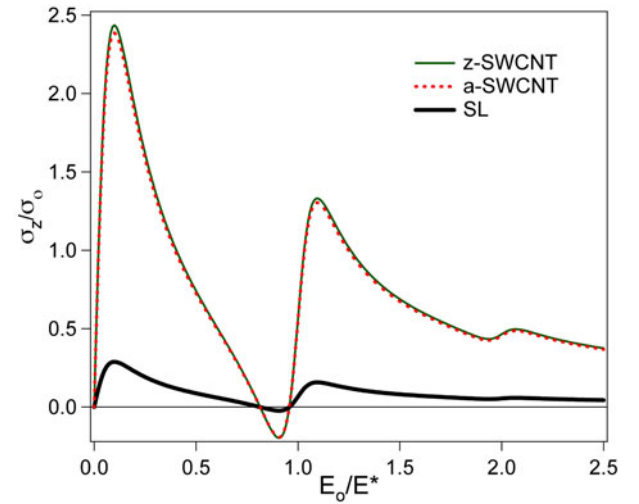
Fig. 3. $\sigma_z/\sigma_0 - E_0/E^*$ curves for for the superlattice (SL, thick solid black curve), the (10,10) armchair SWCNT (a-SWCNT, red dotted curve), and the (12,0) zigzag SWCNT (z-SWCNT, green thin solid curve) using $\tau = 3 \times 10^{-12}$ s and $T = 287.5$ K.

the SL. This indicates a stronger effective suppression of the current instability in SWCNTs.

The dependence of j_z on E_0 (Eq. (17)) as well as σ_z (Eq. (18)) on E_0 arise under the action of strong ac field. When ac field is applied along the SWCNT axis in addition to the dc field, new transport channels are opened at large ac fields which are seen as distinctive peaks in the current density and the conductivity characteristics as shown in Figures 2 and 3, respectively. We noted a very steep positive slope in the neighborhood of the maximum electric field, which indicates that the differential conductivity is positive (PDC) in this region (Fig. 2). The PDC is considered one of the conditions for electric stability in the nonlinear system. The negative ac conductivity at the drive frequency ω appears when electric field

is weak. We observed that in the nonlinear regime with high-enough frequency, the dc differential conductivity is positive, while the large-signal high frequency differential conductivity remains negative (Fig. 3), which can be used for THz gain.

The magnitude of the current density as well as the dc differential conductivity is an order of magnitude higher in the armchair SWCNT (10,10) and the zigzag SWCNT (12,0) in comparison to that of the SL. The strong effects in the CNTs are due to the higher density of free electrons in the CNTs. The mechanism of the nonlinearity in CNTs is due to the presence of the high stark components (summation with respect to r, Eqs. (16)−(18)) [14] which are absent in SL, equation (19) [27].

In conclusion, we have used the semi-classical Boltzmann transport equation to obtain the electric current density and the dc conductivity in an achiral SWCNTs (armchair (10,10) and zigzag (12,0)) under the influence of simultaneous dc-ac electric fields applied parallel to the tube axis. Our analysis on the current density versus electric field characteristics demonstrate negative frequency differential conductivity resonance enhancement, photon assisted peaks, suppression of current instability induced by negative dc conductivity and therefore the possibility of terahertz gain at room temperature without electric instabilities.

References

1. G.Ya. Slepyan et al., Phys. Rev. A **60**, 777 (1999)
2. P.H. Siegel, IEEE Trans. Microwave Theor. Tech. **50**, 910 (2002)
3. M. Tonouchi, Nat. photon. **1**, 97 (2007)
4. T. Hyart, K.N. Alekseev, E.V. Thuneberg, Phys. Rev. B **77**, 165330 (2008)
5. A.W.M. Lee et al., Opt. Lett. **19**, 2840 (2007)
6. B. Ferguson, X.C. Zhang, Nat. Mater. **1**, 26 (2002)
7. G.Ya. Slepyan et al., Phys. Rev. A **63**, (2001) 053808
8. D. Dragoman, M. Dragoman, Physica E **25**, 492 (2005)
9. M. Dragoman et al., Appl. Phys. Lett. **88**, 073503 (2006)
10. G.Ya. Slepyan et al., Phys. Rev. B **73**, 195416 (2006)
11. S.A. Maksimenko, G.Y. Slepyan, Phys. Rev. Lett. **84**, 362 (2000)
12. G. Pennington et al., Phys. Rev. B **68**, 045426 (2003)
13. J.M. Xu, Infrared Phys. Technol. **42**, 485 (2001)
14. R. Saito, G. Dresselhaus, M.S. Dresselhaus, *Physical Properties of Carbon Nanotubes* (Imperial College Press, London, 1998)
15. V.I. Margulis et al., Physica B **245**, 173 (1998)
16. J.M. Xu, Infrared Phys. Technol. **42**, 485 (2001)
17. K.G. Batrakov et al., J. Nanophoton. **4**, 041665 (2010)
18. M.J. Hagmann, IEEE Trans. Nanotechnol. **4**, 289 (2005)
19. Y.T. Dai et al., J. Comput. Theor. Nanosci. **5**, 1372 (2008)
20. G.Ya. Slepyan et al., Phys. Rev. B **81**, 205423 (2010)
21. C. Staneiu et al., Appl. Phys. Lett. **81**, 4064 (2002)
22. S.S. Abukari, S.Y. Mensah, N.G. Mensah, K.A. Dompreh, A. Twum, F.K.A. Allotey, Direct current generation due to wave mixing in zigzag carbon nanotubes, `arXiv:1007.1772v1`
23. S.A. Maksimenko, G.Ya. Slepyan, in *Proceedings of the 8th International Conference on Electromagnetics of Complex Media, Lisbon, Bianisotropics 2000,* pp. 249–252
24. S.A. Ktitorov et al., Sov. Phys. Solid State **13**, 1872 (1972)
25. H. Kroemer, Large-amplitude oscillation dynamics and domain suppression in a superlattice Bloch oscillator, `arXiv:cond-mat/0009311v1`
26. C. Kane, L. Balents, M.P.A. Fisher, Phys. Rev. Lett. **79**, 5086 (1997)
27. K.N. Alekseev et al., Phys. Rev. Lett. **80**, 2669 (1998)